

# Target spiking patterns enable efficient and biologically plausible learning for complex temporal tasks

Paolo Muratore<sup>1\*</sup> , Cristiano Capone<sup>2</sup> , Pier Stanislao Paolucci<sup>2</sup>

**1** SISSA – International School for Advanced Studies, Trieste, Italy

**2** INFN, Sezione di Roma, Rome, Italy

 These authors contributed equally to this work.

\* pmurator@sissa.it

## Abstract

Recurrent spiking neural networks (RSNN) in the human brain learn to perform a wide range of perceptual, cognitive and motor tasks very efficiently in terms of energy consumption and requires very few examples. This motivates the search for biologically inspired learning rules for RSNNs to improve our understanding of brain computation and the efficiency of artificial intelligence. Several spiking models and learning rules have been proposed, but it remains a challenge to design RSNNs whose learning relies on biologically plausible mechanisms and are capable of solving complex temporal tasks. In this paper, we derive a learning rule, local to the synapse, from a simple mathematical principle, the maximization of the likelihood for the network to solve a specific task. We propose a novel target-based learning scheme in which the learning rule derived from likelihood maximization is used to mimic a specific spiking pattern that encodes the solution to complex temporal tasks. This method makes the learning extremely rapid and precise, outperforming state of the art algorithms for RSNNs. We demonstrate the capacity of our model to tackle several problems like learning multidimensional trajectories and solving the classical temporal XOR benchmark. Finally, we show that an online approximation of the gradient ascent, in addition to guaranteeing complete locality in time and space, allows learning after very few presentations of the target output. Our model can be applied to different types of biological neurons. The analytically derived plasticity learning rule is specific to each neuron model and can produce a theoretical prediction for experimental validation.

## Introduction

The development of biologically inspired and plausible neural networks has a twofold interest. On the one hand, neuroscience aims to achieve a better understanding of the functioning of biological intelligence. On the other hand, machine learning (e.g. deep learning [1]) tries to borrow secrets from biological networks. To justify the search for biological learning principles it is enough to consider that the human brain works with only 20 watt.

The transmission of information through spikes is a widespread feature in biological networks and is believed to be a key element for efficiency in energy consumption and for the detection of causal relations between events. Spike-timing-based neural codes are experimentally suggested to be important in several brain systems. In the barn owl auditory system, for example, coincidence-detecting neurons receive temporally precise

spike signals from both ears [2]. In humans, precise timing of first spikes in tactile afferents encodes touch signals at the fingertips [3]. If the same touch stimulus is repeated several times, the relative timing of action potentials is reliably reproduced [3]. Similar coding have also been suggested in the rat’s whisker response [4] and for rapid visual processing [5].

Because of the enormous biological relevance of spike-time-based coding, in the last years different spiking network models have been proposed, for feedforward networks [6–10] and even for recurrent ones [11–15].

However, the capture of long-time temporal dependence on backpropagation-based techniques is computationally expensive and leads to synaptic updating rules that are difficult to frame in a biological substrate. Target-based learning frameworks [13, 14], as opposed to error-based [11, 16], bypass the issue of biologically implausible error back-propagation by providing to the network a target activity to mimic.

In this work, we provide a theoretical framework based on maximum likelihood techniques [17, 18] for target-based learning in biological recurrent networks. We show that the introduction of a likelihood measure as objective function is sufficient to derive biologically realistic target-based synaptic updating rules. Other papers have proposed a similar probabilistic framework for spiking networks [19–21] but they mainly aimed to train the network to reproduce specific patterns of spikes.

Here we propose a target-based learning protocol that assigns to the RSNN a specific internal spike coding for the solution of a task, instead of looking for a solution among those in a huge space of possible alternatives, as error-based approaches would do. This allows our model to achieve a tremendous efficiency in learning. In addition, our approach results quite natural in terms of biological plausibility. Indeed it does not require the assumption of error propagation in the cortex, which is not yet a solid feature in terms of experimental observations. Rather, we rely on the presence of the so termed ‘referent activity templates’ which are spike patterns generated by neural circuits present in other portions of the brain, which are to be mimicked by the network subjected to learning [22, 23]. Also, the learning rule emerging from our likelihood-based framework results to be biologically plausible because it is local to the synapse, namely it does not require the evaluation of global observables over multiple neurons or multiple times.

We use our learning protocol to train an RNN to solve 3 different tasks. First, we train the network to reproduce 3D trajectories. We achieved an error which is lower than e-prop1 [11] and than the biologically unfeasible BPTT. Second, we trained the network to reproduce a high dimensional (56 dimensions) walking dynamics trajectory [24], showing that it is able both to learn the sequence and to display a spontaneous walking pattern beyond the learned epoch. Third, we demonstrate that our model is able to solve the classical temporal XOR task.

In order to define a learning rule which is completely local in space and time we perform what is call the online approximation [20], which demonstrates to be extremely beneficial to the training velocity when learning from a small number of presentations.

## Results

### Target-based training protocol

We considered a target-based approach which conceptualizes learning as the successful replay of a target dynamics  $\mathbf{s}_{\text{targ}} = \{\mathbf{s}_{\text{targ}}^t\}$ . A very important point is the way such  $\{\mathbf{s}_{i,\text{targ}}^t\}$  is defined. Compared to unsupervised or reward-based learning paradigms, supervised paradigms on the level of single spikes might appear less relevant from a biological point, since it is questionable what type of signal could tell the neuron about

the target spiking sequence. Here we propose a biologically plausible way to generate such target. The neurons in the RSNN to be trained receive an input  $\mathbf{I}_{\text{teach}}^t$  from neurons belonging to another population of neurons, e.g. from other cortical areas [15, 25].  $\mathbf{I}_{\text{teach}}^t$  shapes the probability of firing, contributing to defining the target spiking sequence  $s_{i,\text{targ}}^t$ . Let's now suppose that the teaching signal is a function (e.g. the linear function  $\mathbf{I}_{\text{teach}}^t = \mathbf{J}_{\text{teach}} \mathbf{y}^{\text{in}}$ ) of the activity  $\mathbf{y}^{\text{in}}$  of other areas. The objective of our protocol is to train the network to produce a target readout  $\mathbf{y}^{\text{targ}} = \mathbf{J}_{\text{out}} \mathbf{s}_{\text{targ}}$ , in principle accessible to another area of the brain. In conclusion the training phase is obtained under the influence of  $\mathbf{y}^{\text{in}}$  coming from some areas (e.g. a visual sequence in the visual cortices), while in the retrieval the network is autonomously able to provide the output signal  $\mathbf{y}^{\text{targ}}$  (e.g. a motor sequence in the motor cortices). It is a quite natural hypothesis that the input is a function of target output  $\mathbf{y}^{\text{in}} = F(\mathbf{y}^{\text{targ}})$  (and viceversa). In this work we consider the simplest scenario where  $\mathbf{y}^{\text{in}} = \mathbf{y}^{\text{targ}}$ , as represented in Fig.1A where  $\mathbf{J}_{\text{teach}}$  projects the  $\mathbf{y}^{\text{targ}}$  signal.

The importance for the choice of a specific internal coding  $\{s_{i,\text{targ}}^t\}$  can be clarified after considering the alternative error-based approach [11]. In that case, the space of the solution is extremely high, namely a large number of different internal coding are capable to solve the task. On the other hand, the choice for the specific internal solution  $\{s_{i,\text{targ}}^t\}$  makes the learning extremely faster. Such formalism can be applied to accomplish different temporal tasks. Some of them are described below.

## Network model and learning algorithm

We propose a network of spiking neurons described by the real-valued variable  $v_j^t \in \mathbb{R}$ , their membrane potential, where the  $j \in \{1, \dots, N\}$  label identifies the neuron and  $t \in \{1, \dots, T\}$  is a discrete time index. Each neuron exposes an observable state  $s_j^t \in \{0, 1\}$ , which represents the occurrence of a spike from neuron  $j$  at time  $t$  and it is randomly generated as a function of the membrane potential  $p(s_j^t | v_j^t) = g(s_j^t, v_j^t)$ . We use  $\mathbf{v}^t = \{v_j^t\}$  and  $\mathbf{s}^t = \{s_j^t\}$  to indicate the collections of internal and observable network states.

Assuming a synchronous update dynamics, the likelihood of a target sequence of spikes  $\{\mathbf{s}_{\text{targ}}^t\}$  can be easily written as the product over all times and neurons of the probability  $p(s_{j,\text{targ}}^t | v_j^t)$ . Thus the log-likelihood of the network activity  $\mathbf{s}_{\text{targ}}$  can be introduced as:

$$\begin{aligned} \mathcal{L}(\mathbf{s}_{\text{targ}}; \mathbf{J}) &= \log p(\mathbf{s}_{\text{targ}}; \mathbf{J}) = \log \prod_{t=1}^T \prod_{i=1}^N p\left(s_{i,\text{targ}}^{t+1} | \mathbf{v}^t, \mathbf{s}_{\text{targ}}^t; \mathbf{J}\right) = \\ &= \sum_{t=1}^T \sum_{i=1}^N \log p\left(s_{i,\text{targ}}^{t+1} | \mathbf{v}^t, \mathbf{s}_{\text{targ}}^t; \mathbf{J}\right) \end{aligned} \quad (1)$$

where  $\mathbf{J}$  is the collection of parameters that are used in the computation. The probability of spike generation can be written as:

$$p(\mathbf{s}^{t+1} | \mathbf{v}^t) = \frac{\exp \mathbf{s}^{t+1} \left( \frac{\mathbf{v}^t - v^{th}}{\delta v} \right)}{1 + \exp \left( \frac{\mathbf{v}^t - v^{th}}{\delta v} \right)} \quad (2)$$

where  $v^{th}$  is the firing threshold and  $\delta v$  defines the amount of noise in the spike generation. In the  $\delta v \rightarrow 0$  limit the generation is deterministic and  $p(\mathbf{s}^{t+1} | \mathbf{v}^t) = \Theta(\mathbf{v}^t - v^{th})$ . This was indeed the limit in which we performed the numerical experiments presented in this paper.

## Learning rule for cuBa neurons

Without loss of generality (see the section dedicated to conductance based neurons) we now assume for simplicity that the neuron integrates its input as a current-based (cuBa) leaky integrate and fire (LIF) neuron which dynamics evolves obeying the following equation:

$$\mathbf{v}^t = \left(1 - \frac{\Delta t}{\tau_m}\right) \mathbf{v}^{t-1} + \frac{\Delta t}{\tau_m} (\mathbf{J} \hat{\mathbf{s}}^{t-1} + \mathbf{I}^t) \quad (3)$$

Where  $\Delta t$  is the time integration step,  $\tau_m$  is the membrane time constant,  $\mathbf{J} \in \mathbb{R}^{N \times N}$  is the recurrent network matrix that defines the synaptic connections within our model, while  $\mathbf{I}^t$  is a general external input.

We also assumed that the spikes undergoes an exponential synaptic filtering with a time scale  $\tau_s$ .  $\hat{\mathbf{s}}^t$  is the filtered spike signal and is expressed as:

$$\hat{\mathbf{s}}^t = \left(1 - \frac{\Delta t}{\tau_s}\right) \hat{\mathbf{s}}^{t-1} + \frac{\Delta t}{\tau_s} \mathbf{s}^t \quad (4)$$

The derivation can be generalized to different choices of synaptic filtering kernels (e.g. alpha function). To make the recurrent network reliably reproduce the target pattern of activity we need to maximize the likelihood for the system to express the dynamics defined by  $\mathbf{s}_{\text{targ}} = \{s_{i,\text{targ}}^t\}$ . We refer to such likelihood as  $\mathcal{L}(\mathbf{s}_{\text{targ}}; \mathbf{J})$  where  $\mathbf{J}$  are the recurrent synaptic weights of the system. This can be achieved by a gradient based algorithm, which suggests that the optimal plasticity rule is a weight update proportional to the likelihood gradient (see Methods section for derivation):

$$\Delta J_{ij} \propto \frac{\partial \mathcal{L}(\mathbf{s}_{\text{targ}}; \mathbf{J})}{\partial J_{ij}} = \sum_{t=1}^{T-1} \left[ s_{i,\text{targ}}^{t+1} - s_{i,\text{pred}}^{t+1} \right] \frac{\partial v_i^t}{\partial J_{ij}} \quad (5)$$

$s_{i,\text{pred}}^t$  is the activity predicted by the network without the teaching signal. This stands in the  $\delta v \rightarrow 0$  limit (see Methods for details). It is worth underlining the peculiar form of the obtained expression (Eq.5), which is remarkably similar to the form obtained in [26], where the first term in the left parenthesis can be regarded as an instantaneous prediction error: at each time step the target and spontaneous activity are compared and a learning signal is produced.

The second factor  $\frac{\partial v_i^t}{\partial J_{ij}}$  represents what is referred to in the literature as the spike response function [26]: it uses the information of the target trajectory to enable learning only for synapses which are causally related to recent pre-synaptic activity.

## Learning to generate 3D trajectories

To test the performances of a system governed by the derived learning rule we first tackle the standard three-dimensional temporal pattern generation task.

The task definition is the following: given an input signal  $\mathbf{I}_{\text{clock}}^t$  (which we refer to as clock), the network is asked to produce an output target signal through a linear readout of the internal spiking activity. Namely the system is asked to learn a temporal input-output relationship between the clock signal and the target trajectory.

The target output  $\mathbf{y}_{\text{targ}}^t \in \mathbb{R}^3$  is a temporal pattern composed of 3 independent continuous signals. Each target signal is specified as the superposition of the four frequencies  $f \in \{1, 2, 3, 5\}$  Hz with uniformly extracted random amplitude  $A \in [0.5, 2.5]$  and phase  $\phi \in [0, 2\pi]$ . The network is also supposed to receive a clock-like input signal  $\mathbf{I}_{\text{clock}}^t = \mathbf{J}^{\text{in}} \mathbf{x}_{\text{clock}}^t$ , where  $\mathbf{J}^{\text{in}} \in \mathbb{R}^{N \times K}$  and  $\mathbf{x}_{\text{clock}}^t \in \mathbb{R}^K$ .

For this task we equip our recurrent network with a standard linear read-out layer  $\mathbf{y}^t = \mathbf{J}^{\text{out}} \mathbf{s}^t$ , where  $\mathbf{J}^{\text{out}} \in \mathbb{R}^{3 \times N}$  and  $\mathbf{s}^t \in \{0, 1\}^N$ .

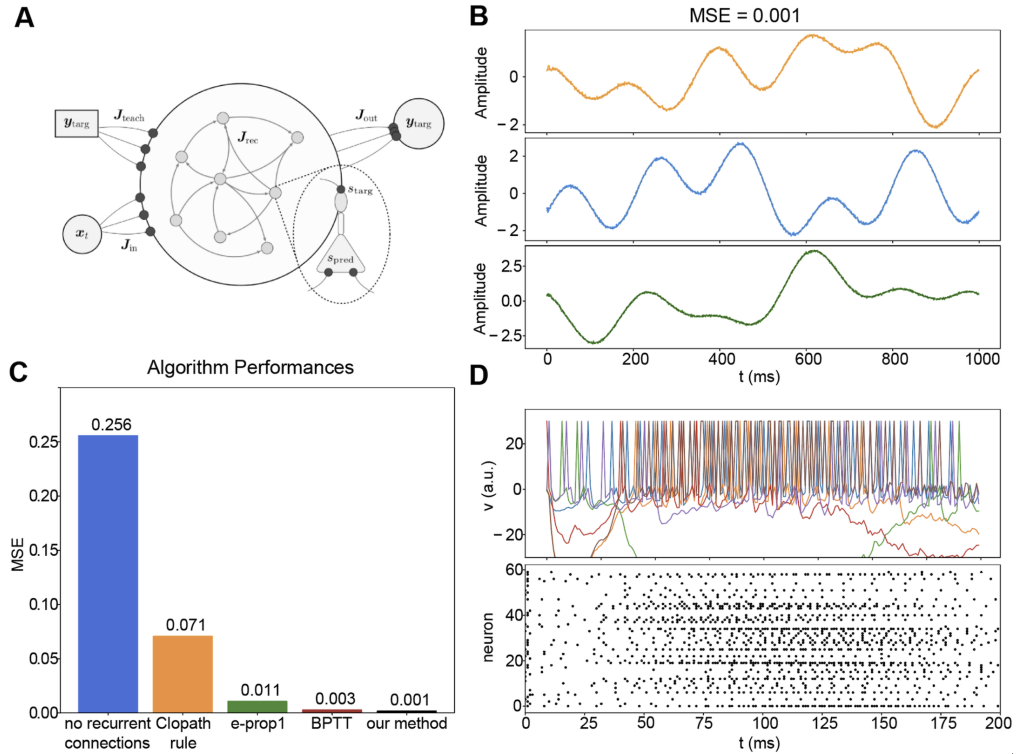


**Fig 1. Results for the Pattern Generation task.** **A)** Graphical representation of the system’s architecture. Each recurrent neuron can be thought of as a two-compartment neuron where the basal region stores the neuron state, while in the apical part the teaching input is received: the resulting learning signal is the different between this two quantities. The recurrent activity is then decoded via a linear readout layer with three output neurons, one for each trajectory. **B)** Generated temporal trajectories. Dashed lines report the target signal, while the continuous curves represent the system generated temporal patterns as decoded by the trained linear readout layer. An overall MSE (Mean Squared Error) of  $MSE = 0.001$  was achieved. **C)** Comparison of different learning algorithms on the Pattern Generation Task as reported in [11]. Learning performances are evaluated as final MSEs. The blue bar represents the final MSE when only the readout layer is trained, thus no recurrent synapses optimization is performed. Performances of the Clopath [27] learning rule, as well as E-prop1 and Back-Propagation-Through-Time (BPTT), are reported with the corresponding final MSE. It is thus shown how our algorithm significantly improves performances on this particular task. **D)** Representation of recurrent network activity. In the upper plot the dynamics of the internal state of six neurons randomly extracted from the network population is reported over time. The lower raster plot presents the activity of a population of 60 neurons from the completed network. Only the first 200 temporal steps of the complete simulations are reported for clarity reasons. The simulation used a network of  $N = 500$  neurons and a total simulation time of  $T = 1000$  time steps.

The idea is to construct an internal target pattern of activity  $\{s_{i,targ}^t\}$  for the spiking network that contains the relevant information needed to solve the task, namely a pattern that encodes the target signal. The readout layer is then trained to decode such information from the target pattern using standard optimization techniques (MSE objective function with Adam optimizer), while the recurrent network exploits the maximum-likelihood training procedure to adjust its synaptic matrix  $\mathbf{J}$  to generate a

recurrent signal that, together with the clock-like input  $\mathbf{I}_{\text{clock}}^t$ , results in the desired temporal pattern.

To produce a valuable target network activity we use the untrained network and record its spontaneous activity when subject to an input  $\mathbf{I}^t = \mathbf{I}_{\text{clock}}^t + \mathbf{I}_{\text{teach}}^t + \mathbf{I}_0$  composed of the clock-like term  $\mathbf{I}_{\text{clock}}^t = \mathbf{J}_{\text{clock}}^{\text{in}} \mathbf{x}^t$ , a random projection of the target signal  $\mathbf{I}_{\text{teach}}^t = \mathbf{J}_{\text{teach}}^{\text{in}} \mathbf{y}_{\text{targ}}^t$  and  $\mathbf{I}_0$ , a constant current. We assume that  $\mathbf{I}_0 = I_0$  is the same for all the neurons and it is chosen in order to have the firing rate of the neurons in a suitable range. In this scenario both  $\mathbf{J}_{\text{clock}}^{\text{in}}$  and  $\mathbf{J}_{\text{teach}}^{\text{in}}$  are static random Gaussian matrix with zero mean and variance  $\sigma_{\text{in}}$  and  $\sigma_{\text{teach}}$ . Our choice was to set the teach  $\mathbf{I}_{\text{teach}}^t$  and the clock current  $\mathbf{I}_{\text{clock}}^t$  at comparable order of magnitudes (see Tab.1 for the number of neurons and the other parameters used for this task).

We observe that the matrix  $\mathbf{J}_{\text{teach}}^{\text{in}}$  contribute to define the internal target pattern  $\{s_{i,\text{targ}}^t\}$  since it induces such internal dynamics. The network is asked to learn to autonomously reproduce the target internal dynamics  $\{s_{i,\text{targ}}^t\}$  by using the recurrent synapses  $\mathbf{J}$  and the clock signal  $\mathbf{I}_{\text{clock}}^t$  in absence of the teaching signal  $\mathbf{I}_{\text{teach}}^t$ . This is achieved through the likelihood maximization, and the weight updates expressed in the previous section. Also the readout weight are trained with a standard minimization of the error function (see Methods section for details).

In the retrieval phase the plasticity is turned-off and the clock current is provided to the network. The spiking generated activity is decoded by the linear readout, and such output is compared to the target trajectory by evaluating the mean square error (MSE).

The system is very efficient to solve the task, interestingly after only 25 steps of a gradient ascent optimizer the system was able to reproduce the trajectory with an error Mean Squared Error  $\text{MSE} = 0.02$ . In Fig.1 we reported the results for the Pattern Generation task. After 1000 iterations of the Adam optimizer the system achieved a final Mean Squared Error  $\text{MSE} = 0.001$ , computed across the three-dimensional output (Fig.1B). The activity of the internal neuron state  $\mathbf{v}^t$ , is reported over time, together with a raster plot of the recurrent network activity (Fig.1D). It is relevant to stress that the obtained performances are significantly better with respect to competing alternative algorithms for spiking neural networks learning temporal sequences. A quantitative comparison of performances, measured as final MSEs, is reported in the bar plot of Fig.1C.

We remark that for this specific task the clock signal is not necessary. Indeed the network is able to learn the following steps in the dynamics as a function of the previous ones. In test phase the trajectory can be completely retrieved by providing the suitable initial condition to the network. Our choice to use the clock is taken in order to reproduce exactly the same conditions proposed in the benchmark reported in [11, 12].

## Walking dynamics

In this task we challenge our proposed framework to successfully address a complex real-world scenario. The quest is to elaborate the problem of learning a realistic multi-dimensional temporal trajectory. We addressed the benchmark problem [14, 28, 29] of learning the walking dynamics of a humanoid skeleton composed of 31 joints (head, femur etc...) each of which endowed of peculiar rotational degrees of freedom  $\boldsymbol{\theta}(t)$ . For example the femur can in principle express rotations on three different axes  $\boldsymbol{\theta}_{\text{femur}} \in \mathbb{R}^3$ , while the wrist is constrained to rotate just around a single axis  $\theta_{\text{wrist}} \in \mathbb{R}$ . Joints are moreover considered unstretchable, so the set of rotations  $\Theta = \{\boldsymbol{\theta}_{\text{joint}}(t)\}$  completely defines the system. The total number of temporal trajectories that our network needs to control is given by the total number of degrees of freedom of the system, which in our problem evaluates to  $D = 56$ . Data used in this task are obtained from the database developed in [24].

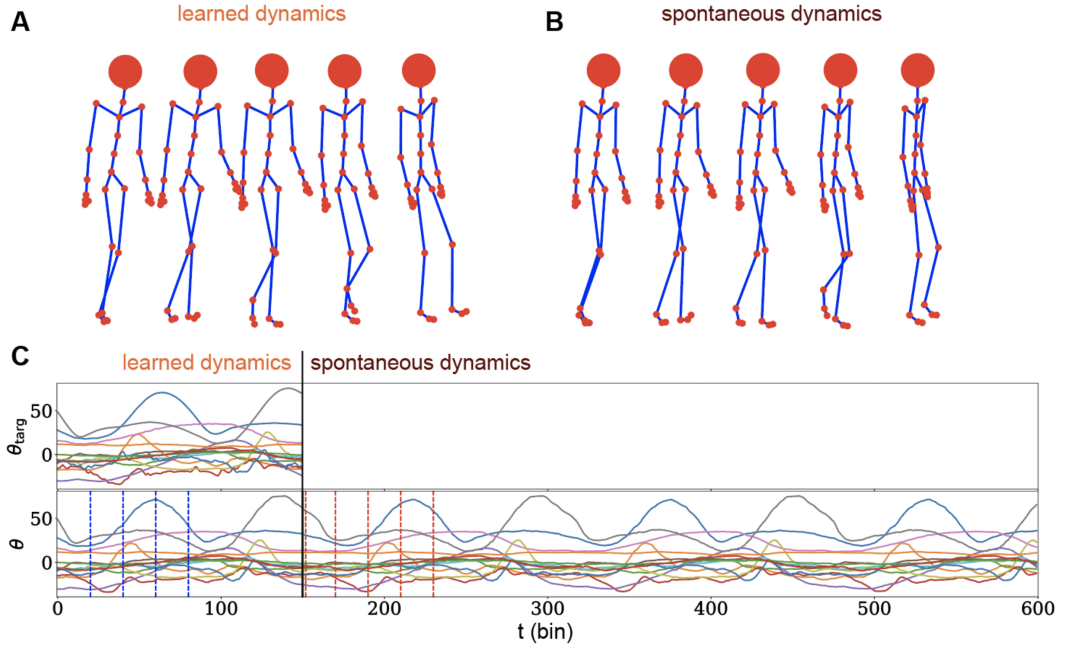


**Fig 2. Walking Dynamics.** **A)** Three-dimensional reconstruction of the walking dynamics produced by the network activity. Reported frames corresponds to  $t = \{0, 20, 40, 60, 80\}$ . **B)** Three-dimensional reconstruction of the spontaneously generated walking dynamics after the end of the learned-by-memory trajectory. A different, but plausible and exactly periodical behaviour emerges, indicating that the system has successfully learnt how to construct and independent walking cycle. Frames shown corresponds to  $t = \{150, 170, 190, 210, 230\}$ . **C)** Collection of 15 out of the 56 temporal angular trajectories for both the target motion (upper plot) and learnt dynamics (lower plot). The system receives explicit instructions for  $t < 150$  steps, where training is performed. Vertical dotted blue lines highlight the temporal frames reported in panel A. The system then produced a longer, spontaneous dynamics for  $t \in [150, 600]$ . Vertical red dotted lines highlight the spontaneous activity frames reported in panel B.

An interesting property of the walking dynamics is indeed its periodicity (data is however derived from motion capture techniques that invalidate exact periodicity). It is thus interesting to explore if the network, trained on a single cycle, is capable of correctly generalize the learnt dynamics by producing novel, plausible, walking behaviour.

The protocol used for this task is exactly the same presented in Learning 3D Trajectories section, with the only difference of the dimension of the trajectory to be learned which is  $D = 56$  instead of 3. From this follow that the input matrix  $\mathbf{J}_{\text{teach}} \in \mathbb{R}^{N \times D}$  and that the output layer is composed of  $D$  neurons. The network parameters for this task are defined in Table.1 for details. Results of the described procedure are reported in Fig.2.

The network successfully memorizes and retrieves the target dynamics with a very small error (MSE = 0.026 on normalized trajectories) after 250 iterations of Adam Optimizer (Fig.2A and Fig.2C up to  $t = 150$ ). Also we let the model generate the trajectory after the end of the learned one. Interestingly the network is capable to generate spontaneously a plausible almost periodic dynamics (Fig.2B and Fig.2C from  $t = 150$  on).

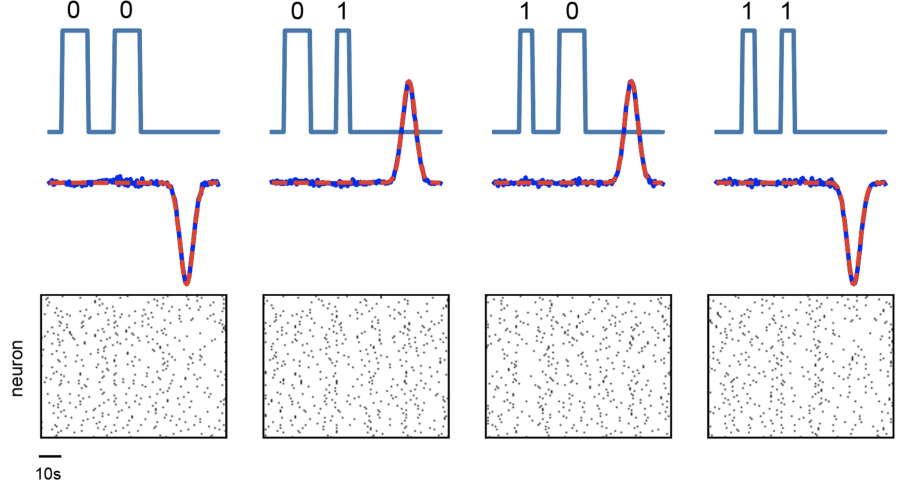


**Fig 3. Results for the temporal XOR test.** The four possible inputs combinations of the binary temporal XOR operation are reported together with the produced output response of the system. (top) On the upper part of each graph the incoming signals are plotted as a function of time, underlining the temporal structure of the task, where the bit is encoded in the duty cycle of a square wave. On the lower part of the graph both the target and the produced network response activity are reported. Continuous blue lines are used for the retrieved output signals, while dashed red lines represents the desired correct output. (bottom) Rastergam of the related internal spiking activity.

## Temporal XOR

In order to further validate the generality of the proposed learning framework, we assessed the well known temporal XOR task. In this task the system is asked to respond at time  $t_3$  with a non-linear XOR transformation between the bits  $A_{in}^1$  and  $A_{in}^2$  encoded by two input signals  $a_1^t$  and  $a_2^t$  provided at preceding times  $t_1$  and  $t_2$ . They encode the desired bit using the length of the duty cycle of a single pulse square wave: (50%  $\rightarrow$  0, 25%  $\rightarrow$  1). This defines 4 possible input signals  $x_\mu^t = a_1^t + a_2^t$ ,  $\mu \in \{0, 1, 2, 3\}$ . The system target response  $\mathbf{y}_{targ}^t$  is a smooth wave form centered at time  $t_3$  whose amplitude  $A_{out}^3$  encodes the XOR computation of the two inputs:  $A_{out}^3 = 2(A_{in}^1 \oplus A_{in}^2 - 0.5)$ . This particular choice for the definition of the task is to reproduce the protocol described in [14].

The system is trained to generate four internal target sequences  $\mathbf{s}_\mu^{targ}$  on the four possible input combinations. Each sequence is produced by extracting the spontaneous activity of an untrained network receiving as input both the two square-wave signals encoding the bits to be processed  $\mathbf{I}_{bits}^t = \mathbf{J}_\mu^{in} \mathbf{x}_\mu^t$  and, similarly to the previous task, the encoded target response  $\mathbf{I}_{teach}^t = \mathbf{J}_{teach}^{in} \mathbf{y}_{targ}^t$ . We notice that  $\mathbf{I}_{bits}^t$  is the equivalent of the clock current described in the previous tasks. In this task such a current is essential since it provides the input signal, which has to be processed by the network. The projecting matrices  $\mathbf{J}_\mu^{in}$  and  $\mathbf{J}_{teach}^{in}$  are static random Gaussian matrix with zero mean and variance  $\sigma_{in}$  and  $\sigma_{targ}$ . The recurrent network training increases the likelihood of all the four target activities  $\mathbf{s}_\mu^{targ}$  by processing one sequence at a time in random order and performing the maximum-likelihood prescribed updating rule. Concurrently a standard linear readout is trained to decode the four sequences  $\mathbf{s}_\mu^{targ}$  with MSE objective function and standard Adam optimizer with default parameters.

Fig.3 summarizes the outcome of the training procedure on the temporal XOR task: all the four possible inputs combination are correctly handled by the system, which

learns to accurately reproduce the desired signal (see Tab.1 for the number of neurons and the other parameters used for this task).

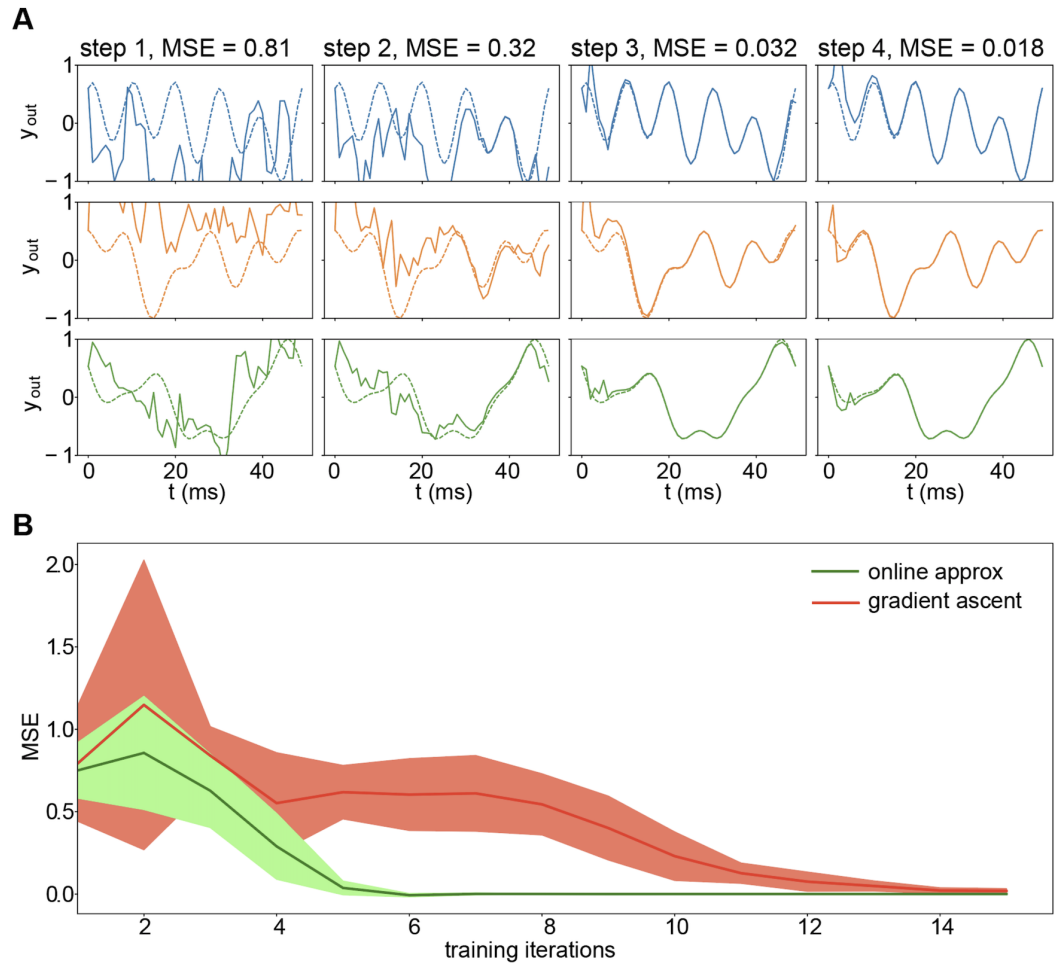


**Fig 4. Learning with a few presentations.** **A)** Columns represent the network output after 1, 2, 3 and 4 learning steps (dashed line: target trajectory, solid line: retrieved trajectory). At the fourth step the network reached an  $MSE = 0.018$ . **B)** Online approximation (green) demonstrates to be faster than standard gradient descent (red). Thick lines and shadings: average and variance over 30 realizations.

### Learning with a few presentations

Fast learning from few examples is a major feature in biological systems. For this reason we show an example in which a trajectory is learned by the system after a very few presentations. The task is the same as the one described in the section *Learning to generate 3D trajectories* with the only difference that here the trajectory is composed of 50 time bins. In Fig.4(top) each column reports the retrieval of the 3D trajectory after a different number of learning iterations (in particular after 1,2,3 and 4 presentations). The target sequence is represented in solid lines, while the retrieved trajectory is in dashed lines.

After only 4 presentations the trajectory is already learned by the spiking network with a very low error.

Such fast learning is achieved when an online version of the gradient ascent is used. This version of the training is an approximation in which the weights are updated at each time bin  $t$  accordingly to the following equation:

$$\Delta J_{ik}^t = \frac{\eta}{\delta v} \left[ s_{i,\text{targ}}^{t+1} - s_{i,\text{pred}}^{t+1} \right] \frac{\partial}{\partial J_{ik}} v_i^t \quad (6)$$

instead of updating them after the whole sequence presentation as expressed in eq.5. We refer to this approximation as the online approximation. This approximation has been shown to be a good approximation of the gradient ascent for small learning rate [20]. On the other side, in order to have a fast learning, the learning rate cannot be too small. Here we show that the online approximation, in addition to be local in time, and then biologically plausible, it is extremely beneficial to the fast learning. We indeed compared the learning for the standard gradient ascent and for the online approximation. The result is reported in Fig.4(bottom panel) respectively in red and green.

The online approximation is much faster. It takes on average 5 presentations to learn the trajectory ( $\text{MSE} < 0.01$ ), three times less than what required by the standard gradient ascent.

## Learning rule for coBa neurons

As mentioned above our approach is general and allows to analytically derive an optimal plasticity rule for different neuronal models. Namely, a different differential equation brings to a different plasticity rule. We already derived such rule for current-based leaky integrate and fire neurons, here we report learning rule for conductance-based neurons. In this case the evolution for its membrane potential is different because the input affect its dynamics in a multiplicative fashion with the membrane potential  $v_i^t$  itself and is described by the following equation:

$$\mathbf{v}^t = \left( 1 - \frac{\Delta t}{\tau_m} \right) \mathbf{v}^{t-1} + \frac{\Delta t}{\tau_m} \left[ (E_{\text{exc}} - \mathbf{v}^{t-1}) \mathbf{J}_{\text{exc}} \hat{\mathbf{s}}_{\text{exc}}^{t-1} + (E_{\text{inh}} - \mathbf{v}^{t-1}) \mathbf{J}_{\text{inh}} \hat{\mathbf{s}}_{\text{inh}}^{t-1} + \mathbf{I}^t \right] \quad (7)$$

Where  $E_{\text{exc}} = 0\text{mV}$  and  $E_{\text{inh}} = -80\text{mV}$  are the reversal potential for excitatory and inhibitory conductances. exc and inh subscripts distinguished between excitatory and inhibitory neurons and synapses. This means that the populations of neurons has to be segregated in excitatory and inhibitory neurons.

Thus the spike response function is different for excitatory and inhibitory weights and are defined iteratively as

$$\nabla_{\mathbf{J}_{\text{exc}}} \mathbf{v}^t = \left( 1 - \frac{\Delta t}{\tau_m} - \mathbf{J} \hat{\mathbf{s}}^{t-1} \right) \nabla_{\mathbf{J}_{\text{exc}}} \mathbf{v}^{t-1} + \frac{\Delta t}{\tau_m} (E_{\text{exc}} - \mathbf{v}^{t-1}) \hat{\mathbf{s}}_{\text{exc}}^{t-1} \quad (8)$$

and

$$\nabla_{\mathbf{J}_{\text{inh}}} \mathbf{v}^t = \left( 1 - \frac{\Delta t}{\tau_m} - \mathbf{J} \hat{\mathbf{s}}^{t-1} \right) \nabla_{\mathbf{J}_{\text{inh}}} \mathbf{v}^{t-1} + \frac{\Delta t}{\tau_m} (E_{\text{inh}} - \mathbf{v}^{t-1}) \hat{\mathbf{s}}_{\text{inh}}^{t-1} \quad (9)$$

The segregation of the network in excitatory and inhibitory neurons requires to pay attention to the constraint that in the optimization the sign of the synapses has to be conserved.

## Discussion

In recent years a wealth of novel training procedures have been proposed for recurrent biological networks, both continuous and spike-based. This work proposes a maximum-likelihood target-based learning framework for recurrent spiking systems. Borrowing from the Machine Learning and in particular Deep Learning community, the aim is to enable learning in complex systems by defining a suitable architecture and an objective function to be optimized, from which the synaptic update rule is derived. Inspired by the stochastic nature of the single neuronal unit, the likelihood of a complete network activity is chosen as the training objective function. In this picture learning in a biological network is understood to be the processes during which the synaptic matrix is adapted to reproduce a target dynamics with high probability. From this simple theoretical assumption explicit synaptic update rules are derived, which offer a clean interpretation of the single terms. This ensures a tight control on the biological realism of the learning rule. The proposed target-based training protocol has been tested on several temporal tasks: learning to generate trajectory with different dimensionalities (a 3D trajectory and a 56D walking dynamics) and the temporal XOR, which is a non-linear classification problem. In the 3D trajectory generation task the proposed target-based algorithm outperformed the state-of-the-art error-propagation-based algorithms, including e-prop 1 [11] and backpropagation through time. Our model relies on two main assumption: the presence of a teaching signal arriving to the recurrent network and the capability of the neuron to evaluate a local error. The teaching signal is important to generate the internal target representation, and it is plausible to assume that is provided by other cortical areas. The local error is evaluated by the single neuron, and is the difference between the tendency of the neuron to produce a spike and the desired spikes defined by the teaching signal. Theoretical models suggest that this signal might be evaluated by a 2 compartment neuron [26]. Alternately, it has been shown that this learning rule together with a time locality constrain results to be very similar to a standard STDP [19].

In the sake of biological plausibility, in order to achieve a complete locality both in space and in time, we proposed what we called the online approximation, which is an update of the weights at every time  $t$ , where only the information available at the current time is used. Namely it is not necessary to wait for the end of the presentation of training example to perform the weight update. Such a time local approximation is extremely advantageous when learning from a small number of examples, increasing significantly the learning velocity.

Different models of neurons lead to different plasticity learning rules. E.g. for conductance based and current based neurons [30,31] different theoretical learning rules are derived in this work. Such diversity is a theoretical prediction and can be verified experimentally.

## Comparison with other models and biological plausibility

The proposed learning protocol improves the biological plausibility of network architectures used in other recent papers [11, 14, 20]). The model described in [11] relies on a random projection of the errors to the network. On the other hand we bet on a random projection of the desired output into the network, while each neuron evaluate a local error which defines the plasticity rule. Our protocol is also computationally efficient since learning requires a calculation of order  $O(N^2 \times T \times P)$  where  $P$  is the number of presentations of the target pattern. The online approximation further decreases the computational cost by reducing the number of required presentations  $P$ . We claim that this protocol, besides the computational efficiency and the achievement of a smaller MSE, it is also more natural from a biological point of view. Indeed it is

very intuitive to imagine that every portion of the cerebral cortex is a recurrent neural network receiving signals from the other cortices. Such hypothesis, which reinforces the necessity of supervised learning, is inspired by the so termed ‘referent activity templates’ which are spike patterns generated by neural circuits present in other portions of the brain, which are to be mimicked by the network subjected to learning [22, 23].

We remark that the analytic formulation to derive our learning rule resembles those proposed in [19, 20, 20, 26], but they mainly focused on training the network to learn specific temporal patterns of spike. Here we integrate such approach with a target-based learning protocol, allowing to solve complex temporal task. This choice is similar to the one described in the full-Force scheme [13, 14]. Although similar, they are not equivalent, indeed the full-Force learning algorithm aims to reproduce the target input current to each neuron. On the other our target is a specific spiking pattern, allowing for precise spike timing coding. Such findings taken together suggest that the capability of a neuron to estimate a local error is beneficial to the learning process. Experimental evidences suggest that [25] single neurons are indeed capable to integrate different stimuli to estimate local errors. In addition to this in [26] it is described a plausible mechanism to achieve such an error in a two-compartment neuron model.

The choice to project the target output into the network during the training makes our learning protocol similar to what proposed in [13, 14]. A major difference is that our learning method relies on optimizing the timing of the spikes emitted by each neuron rather than optimizing the time course of their input current. Such feature is extremely useful to induce a specific spike-timing-based coding.

## Methods

### Theoretical Derivation of the learning rule for cuBa neurons

In our formalism neurons are modeled as real-valued variable  $v_j^t \in \mathbb{R}$ , where the  $j \in \{1, \dots, N\}$  label identifies the neuron and  $t \in \{1, \dots, T\}$  is a discrete time variable. Each neuron exposes an observable state  $s_j^t \in \{0, 1\}$ , which represents the occurrence of a spike from neuron  $j$  at time  $t$ .

We then define the following probabilistic dynamics for our model:

$$\hat{\mathbf{s}}^t = \left(1 - \frac{\Delta t}{\tau_s}\right) \hat{\mathbf{s}}^{t-1} + \frac{\Delta t}{\tau_s} \mathbf{s}^t \quad (10)$$

$$\mathbf{v}^t = \left(1 - \frac{\Delta t}{\tau_m}\right) \mathbf{v}^{t-1} + \frac{\Delta t}{\tau_m} (\mathbf{J} \hat{\mathbf{s}}^{t-1} + \mathbf{I}^t) \quad (11)$$

$$p(\mathbf{s}^{t+1} | \mathbf{v}^t) = \frac{\exp \mathbf{s}^{t+1} \left(\frac{\mathbf{v}^t - \mathbf{v}^{th}}{\delta v}\right)}{1 + \exp \left(\frac{\mathbf{v}^t - \mathbf{v}^{th}}{\delta v}\right)} \quad (12)$$

Where  $\Delta t$  is the discrete time-integration step, while  $\tau_s$  and  $\tau_m$  are respectively the spike-filtering time constant and the temporal membrane constant. Each neuron is a leaky integrator with a recurrent filtered input obtained via a synaptic matrix  $\mathbf{J} \in \mathbb{R}^{N \times N}$  and an external signal  $\mathbf{I}^t$ .  $v^{th}$  is the firing threshold and  $\delta v$  defines the amount of noise in the spike generation. In the  $\delta v \rightarrow 0$  limit the generation is deterministic and  $p(\mathbf{s}^{t+1} | \mathbf{v}^t) = \Theta(\mathbf{v}^t - v^{th})$ . The log-likelihood of a complete network activity  $\mathbf{s}$  can be expressed as:

$$\mathcal{L}(\mathbf{s}; \mathbf{J}) = \log p(\mathbf{s}; \mathbf{J}) = \log \prod_{t=1}^T \prod_{i=1}^N p(s_i^{t+1} | \mathbf{v}^t, \mathbf{s}^t; \mathbf{J}) = \sum_{t=1}^T \sum_{i=1}^N \log p(s_i^{t+1} | \mathbf{v}^t, \mathbf{s}^t; \mathbf{J}) \quad (13)$$

Where we assumed the parallel update of all the neurons at each time step, and that the probabilistic generation of the spike is independent between neurons at the same time step. Indeed our noisy generation is equivalent to the presence of a source of noise not explicitly described in the system. A possible example is an external source of noise for each neuron. Our description doesn't account for correlated sources of noise.

We notice that in order to evaluate such likelihood it is important to be able to evaluate the membrane potential at each time  $t$ . In order to do so it is necessary to know the spikes  $\mathbf{s}^t$  produced by the network, the law of evolution of the membrane potential (see eq.(11)) and its initial condition  $\mathbf{v}^{t=1}$  (which we usually define as a constant  $v^0$ ).

The idea now is to exploit the introduced likelihood  $\mathcal{L}(\mathbf{s}; \mathbf{J})$  as a valuable tool for a target-based learning. We introduce a target activity  $\mathbf{s}_{\text{targ}}$  and exploit the dependence of the likelihood on the recurrent weights  $\mathbf{J}$  to increase the likelihood of observing the target pattern as the system's spontaneous activity. In particular we compute:

$$\nabla_{\mathbf{J}} \mathcal{L}(\mathbf{s}_{\text{targ}}; \mathbf{J}) = \sum_{t=1}^T \nabla_{\mathbf{J}} \log p(\mathbf{s}_{\text{targ}}^t | \mathbf{v}^{t-1}, \mathbf{s}^{t-1}; \mathbf{J}) \quad (14)$$

This framework thus prescribes to implement as a viable learning rule the likelihood gradient  $\nabla_{\mathbf{J}} \mathcal{L}$ . Via this optimization protocol, the system learns to exploit its resources to encode the desired activity.

The maximum likelihood learning rule then prescribes:

$$\frac{\partial \mathcal{L}}{\partial J_{ik}} = \frac{1}{\delta v} \sum_{t=1}^T \sum_j^N \left[ s_{j,\text{targ}}^{t+1} - \frac{\exp \frac{v_j^t - v^{\text{th}}}{\delta v}}{1 + \exp \frac{v_j^t - v^{\text{th}}}{\delta v}} \right] \frac{\partial}{\partial J_{ik}} v_j^t \quad (15)$$

Where in eq.(15) we have rewritten the likelihood gradient using the index notation. The last term  $\frac{\partial}{\partial J_{ik}} v_j^t$  can be iteratively written by differentiating eq.(11):

$$\frac{\partial}{\partial J_{ik}} v_j^{t+1} = \left( 1 - \frac{\Delta t}{\tau_m} \right) \frac{\partial}{\partial J_{ik}} v_j^{t+1} + \frac{\Delta t}{\tau_m} \hat{s}_{k,\text{targ}}^{t-1} \delta_{ij} \quad (16)$$

and setting an initial condition, e.g.  $\frac{\partial v_j^{t=1}}{\partial J_{ik}} = 0$ . We stress that the differential operator  $\nabla_{\mathbf{J}}$  is only applied to  $\mathbf{v}^{t-1}$  and not to  $\hat{\mathbf{s}}_{\text{targ}}^{t-1}$ , because the latter represents the desired target dynamics, which is assumed to be fixed throughout the training process and thus expresses no dependence on the synaptic matrix  $\mathbf{J}$ . Because of the Kronecher  $\delta$  in eq.(16), together with its initial condition,  $\frac{\partial v_j^t}{\partial J_{ik}}$  differs from zero only when  $j = i$ . We can thus finally write

$$\frac{\partial \mathcal{L}}{\partial J_{ik}} = \frac{1}{\delta v} \sum_{t=1}^T \left[ s_{i,\text{targ}}^{t+1} - \frac{\exp \frac{v_i^t - v^{\text{th}}}{\delta v}}{1 + \exp \frac{v_i^t - v^{\text{th}}}{\delta v}} \right] \frac{\partial}{\partial J_{ik}} v_i^t \quad (17)$$

It follows that the weight plasticity rule can be expressed as

$$\Delta \mathbf{J} = \frac{\eta}{\delta v} \sum_{t=1}^T \left[ \mathbf{s}_{\text{targ}}^t - \frac{\exp \frac{\mathbf{v}^t - \mathbf{v}^{\text{th}}}{\delta v}}{1 + \exp \frac{\mathbf{v}^t - \mathbf{v}^{\text{th}}}{\delta v}} \right]^\top \nabla_{\mathbf{J}} \mathbf{v}^t \quad (18)$$

It is possible to rewrite this expression by recognizing that the second term in the first factor, in the limit  $\delta v \rightarrow 0$  and with  $\eta/\delta v$  finite, represents the network prediction

for the spike vector  $\mathbf{s}_{\text{pred}}^{t+1}$  value at the subsequent time step, based on the current network hidden state  $\mathbf{v}^t$ . Shifting the summed index  $t$  one obtains:

$$\Delta \mathbf{J} = \frac{\eta}{\delta v} \sum_{t=0}^{T-1} [\mathbf{s}_{\text{targ}}^{t+1} - \mathbf{s}_{\text{pred}}^{t+1}]^\top \nabla_{\mathbf{J}} \mathbf{v}^t \quad (19)$$

We note how the obtained expression offers a simple interpretation: it effectively separates into a first learning signal, which is the neuron-wise difference between the teaching signal and the spontaneous network-induced activity, and an eligibility trace.

Using this novel maximum-likelihood framework we have obtained an explicit expression for the synaptic weight update, a result that previously eluded other target-based learning algorithm [13].

## Generation mode

To set the network in generation mode the plasticity is turned off. Then the network is initialized with the proper initial condition  $\mathbf{v}^{t=1} = \mathbf{v}^0$  (which is the same as the one defined in the likelihood maximization protocol), and the evolution dynamics is the one defined in eq.(11) and eq.(12). Once the likelihood is maximized we expect that the system has an high probability to reproduce the desired sequence of spikes  $\mathbf{s}_{\text{targ}}$ .

## Readout training

The training of the readout weights is performed through a standard minimization of the MSE between the output  $\mathbf{y} = \mathbf{J}_{\text{out}} \hat{\mathbf{s}}$  and the target output  $\mathbf{y}_{\text{targ}}$ , which results in the following rule

$$\Delta \mathbf{J}_{\text{out}} = [\mathbf{y}_{\text{targ}} - \mathbf{J}_{\text{out}} \hat{\mathbf{s}}] \hat{\mathbf{s}}^\top \quad (20)$$

Where  $\mathbf{Y}_{\text{targ}} = \{\mathbf{y}_{\text{targ}}^t\}$ ,  $\mathbf{Y}_{\text{targ}} \in \mathbb{R}^{3 \times T}$  is the matrix that collects the target signal over time, while  $\hat{\mathbf{s}} \in \mathbb{R}^{N \times T}$  is the matrix that collects the network observable spikes over time.

## Simulation parameters

We report in the table below the network parameters used in the different tasks.

	3D Trajectories	Temporal XOR	Walking Dynamics	Few Presentations
$N$	500	500	500	500
$T$	1000	130	600	50
$\Delta t$	1 ms	1 ms	1 ms	1 ms
$v_i^0$	$-0.5 \forall i$	$-0.5 \forall i$	$-0.5 \forall i$	$-0.5 \forall i$
$s_i^0$	$s_{i,\text{teach}}^0 \forall i$	$s_{i,\text{teach}}^0 \forall i$	$s_{i,\text{teach}}^0 \forall i$	$s_{i,\text{teach}}^0 \forall i$
$\eta/\delta v$	0.5 (Adam)	0.5 (Adam)	0.5 (Adam)	1.0 (SG-online)
$\delta v$	$\rightarrow 0$	$\rightarrow 0$	$\rightarrow 0$	$\rightarrow 0$
$v^{\text{th}}$	0	0	0	0
$\tau_s$	2 ms	2 ms	2 ms	1.25 ms
$\tau_m$	8 ms	8 ms	8 ms	2 ms
$\sigma_{\text{teach}}$	10	5	10	10
$\sigma_{\text{in}}$	2	3	2	2
$I_0$	-4	-4	-4	-1

**Table 1.** Collection of model parameters used in the various tasks presented in the main text. We have indicated with SG the simple gradient ascent algorithm.

In the 3D trajectory benchmark we used realistic synaptic and membrane timescales, in order to show that we achieved good results with biologically plausible parameters. A smaller membrane timescale usually facilitates the convergence of the method, for this reason we used a shorter time scale in order to further decrease the number of steps required for the learning.

## Acknowledgments

This work has been supported by the European Union Horizon 2020 Research and Innovation program under the FET Flagship Human Brain Project (grant agreement SGA3 n. 945539 and grant agreement SGA2 n. 785907) and by the INFN APE Parallel/Distributed Computing laboratory.

The funders had no role in study design, data collection and analysis, decision to publish, or preparation of the manuscript

## Additional information

The authors declare to have no competing financial and/or non-financial interests in relation to the work described.

## References

1. LeCun Y, Bengio Y, Hinton G. Deep learning. *nature*. 2015;521(7553):436–444.
2. Carr C, Konishi M. A circuit for detection of interaural time differences in the brain stem of the barn owl. *Journal of Neuroscience*. 1990;10(10):3227–3246.
3. Johansson RS, Birznieks I. First spikes in ensembles of human tactile afferents code complex spatial fingertip events. *Nature neuroscience*. 2004;7(2):170.
4. Panzeri S, Petersen RS, Schultz SR, Lebedev M, Diamond ME. The role of spike timing in the coding of stimulus location in rat somatosensory cortex. *Neuron*. 2001;29(3):769–777.
5. Gollisch T, Meister M. Rapid neural coding in the retina with relative spike latencies. *science*. 2008;319(5866):1108–1111.
6. Memmesheimer RM, Rubin R, Ölveczky BP, Sompolinsky H. Learning precisely timed spikes. *Neuron*. 2014;82(4):925–938.
7. Diehl P, Cook M. Unsupervised learning of digit recognition using spike-timing-dependent plasticity. *Frontiers in Computational Neuroscience*. 2015;9:99. doi:10.3389/fncom.2015.00099.
8. Lillicrap TP, Cownden D, Tweed DB, Akerman CJ. Random synaptic feedback weights support error backpropagation for deep learning. *Nature communications*. 2016;7:13276.
9. Zenke F, Ganguli S. Superspike: Supervised learning in multilayer spiking neural networks. *Neural computation*. 2018;30(6):1514–1541.
10. Mozafari M, Ganjtabesh M, Nowzari-Dalini A, Thorpe SJ, Masquelier T. Bio-inspired digit recognition using reward-modulated spike-timing-dependent plasticity in deep convolutional networks. *Pattern Recognition*. 2019;94:87–95.

11. Bellec G, Scherr F, Hajek E, Salaj D, Legenstein R, Maass W. Biologically inspired alternatives to backpropagation through time for learning in recurrent neural nets. 2019; p. 1–37.
12. Nicola W, Clopath C. Supervised learning in spiking neural networks with FORCE training. *Nature communications*. 2017;8(1):2208.
13. DePasquale B, Cueva CJ, Rajan K, Abbott L, et al. full-FORCE: A target-based method for training recurrent networks. *PloS one*. 2018;13(2):e0191527.
14. Ingrosso A, Abbott LF. Training dynamically balanced excitatory-inhibitory networks. *Plos One*. 2019;14(8):e0220547. doi:10.1371/journal.pone.0220547.
15. Capone C, Pastorelli E, Golosio B, Paolucci PS. Sleep-like slow oscillations improve visual classification through synaptic homeostasis and memory association in a thalamo-cortical model. *Scientific Reports*. 2019;9(1):8990.
16. Sacramento Ja, Ponte Costa R, Bengio Y, Senn W. Dendritic cortical microcircuits approximate the backpropagation algorithm. In: Bengio S, Wallach H, Larochelle H, Grauman K, Cesa-Bianchi N, Garnett R, editors. *Advances in Neural Information Processing Systems 31*. Curran Associates, Inc.; 2018. p. 8721–8732. Available from: <http://papers.nips.cc/paper/8089-dendritic-cortical-microcircuits-approximate-the-backpropagation-algorithm.pdf>.
17. Capone C, Gigante G, Del Giudice P. Spontaneous activity emerging from an inferred network model captures complex spatio-temporal dynamics of spike data. *Scientific reports*. 2018;8(1):17056.
18. Capone C, Filosa C, Gigante G, Ricci-Tersenghi F, Del Giudice P. Inferring synaptic structure in presence of neural interaction time scales. *PloS one*. 2015;10(3):e0118412.
19. Pfister JP, Toyozumi T, Barber D, Gerstner W. Optimal spike-timing-dependent plasticity for precise action potential firing in supervised learning. *Neural computation*. 2006;18(6):1318–1348.
20. Jimenez Rezende D, Gerstner W. Stochastic variational learning in recurrent spiking networks. *Frontiers in Computational Neuroscience*. 2014;8:38. doi:10.3389/fncom.2014.00038.
21. Gardner B, Grüning A. Supervised learning in spiking neural networks for precise temporal encoding. *PloS one*. 2016;11(8):e0161335.
22. Knudsen EI. Supervised learning in the brain. *Journal of Neuroscience*. 1994;14(7):3985–3997.
23. Miall RC, Wolpert DM. Forward models for physiological motor control. *Neural networks*. 1996;9(8):1265–1279.
24. Balazia M, Sojka P. Walker-independent features for gait recognition from motion capture data. In: *Joint IAPR International Workshops on Statistical Techniques in Pattern Recognition (SPR) and Structural and Syntactic Pattern Recognition (SSPR)*. Springer; 2016. p. 310–321.
25. Larkum ME. A cellular mechanism for cortical associations: an organizing principle for the cerebral cortex. *Trends in Neurosciences*. 2013;36:141–151.

26. Urbanczik R, Senn W. Learning by the dendritic prediction of somatic spiking. *Neuron*. 2014;81(3):521–528.
27. Clopath C, Büsing L, Vasilaki E, Gerstner W. Connectivity reflects coding: a model of voltage-based STDP with homeostasis. *Nature neuroscience*. 2010;13(3):344.
28. Sussillo D, Abbott LF. Generating coherent patterns of activity from chaotic neural networks. *Neuron*. 2009;63(4):544–557.
29. Alemi A, Machens CK, Deneve S, Slotine JJ. Learning nonlinear dynamics in efficient, balanced spiking networks using local plasticity rules. In: *Thirty-Second AAAI Conference on Artificial Intelligence*; 2018.
30. Capone C, di Volo M, Romagnoni A, Mattia M, Destexhe A. A state-dependent mean-field formalism to model different activity states in conductance based networks of spiking neurons. *bioRxiv*. 2019; p. 565127.
31. di Volo M, Romagnoni A, Capone C, Destexhe A. Biologically realistic mean-field models of conductance-based networks of spiking neurons with adaptation. *Neural computation*. 2019;31(4):653–680.